Retention Kinetics of the ^{18}F-Labeled Sympathetic Nerve PET Tracer LMI1195: Comparison with ^{11}C-Hydroxyephedrine and ^{123}I-MIBG

Rudolf A. Werner[1,2], Christoph Rischpler[3], David Onthank[4], Constantin Lapa[1], Simon Robinson[4], Samuel Samnick[1], Mehrbod Javadi[5], Markus Schwaiger[3], Stephan G. Nekolla[3,6], and Takahiro Higuchi[1,2]

[1]Department of Nuclear Medicine, University of Wuerzburg, Wuerzburg, Germany; [2]Comprehensive Heart Failure Center (CHFC), University of Wuerzburg, Wuerzburg, Germany; [3]Department of Nuclear Medicine, Klinikum rechts der Isar, Technische Universitaet Muenchen, Munich, Germany; [4]Lantheus Medical Imaging, North Billerica, Massachusetts; [5]Division of Nuclear Medicine, Russell H. Morgan Department of Radiology, Johns Hopkins University, Baltimore, Maryland; and [6]German Centre for Cardiovascular Research (DZHK), Partner Site Munich Heart Alliance, Munich, Germany

For correspondence contact: Takahiro Higuchi, Department of Nuclear Medicine/Comprehensive Heart Failure Center, University of Wuerzburg, Oberduerrbacher Strasse 6, 97080 Wuerzburg, Germany.
E-mail: thiguchi@me.com

The importance of the role that the sympathetic nervous system plays in various cardiac disorders, including ischemic heart disease and heart failure, has been well established (*1*). Radionuclide imaging provides a unique technique to noninvasively monitor the local condition of the cardiac sympathetic nervous system in patients. The SPECT imaging agent ^{123}I-metaiodobenzylguanidine (^{123}I-MIBG) is commercially available and has been demonstrated in clinical trials to provide important clinical information for risk stratification in heart failure patients (*2*). However, PET offers improvements over SPECT, namely increased spatiotemporal resolution and well-validated quantification approaches for tissue radiotracer concentrations. The ^{11}C-labeled norepinephrine analog hydroxyephedrine is the most commonly used PET tracer for sympathetic nerve imaging. The superior sensitivity and quantitative capability of ^{11}C-hydroxyephedrine PET allows for reliable assessment of regional neurohumoral abnormalities (*3*). However, the short half-life of ^{11}C (20 min) limits widespread clinical use because of the need for a costly on-site cyclotron.

To overcome the limitations of these conventional tracers, the novel ^{18}F-labeled PET imaging agent ^{18}F-*N*-[3-bromo-4-(3-fluoro-propoxy)-benzyl]-guanidine (^{18}F-LMI1195) has been developed (*4*). It inherits the advantages of ^{18}F-radionuclides, including a longer physical half-life (110 min). An ^{18}F-labeled radiotracer could significantly reduce the cost of tracer production by leveraging delivery systems similar to ^{18}F-FDG used in clinical imaging. Furthermore, the longer half-life can provide more flexibility in study design, allowing for delayed or prolonged imaging. Yu et al. initially characterized ^{18}F-LMI1195 for cardiac neuronal imaging (*4*). The high affinity and specificity of ^{18}F-LMI1195 for the neuronal norepinephrine transporter (NET) were confirmed with a cell membrane binding assay. The feasibility of in vivo imaging with targeting of neuronal NETs at the presynaptic level was demonstrated using a combination

of rabbits and nonhuman primate models. Furthermore, minimal liver uptake in comparison to other conventional nerve tracers was suggested in the animal experiments and is preferable for assessment of the left ventricular inferior wall. Most recently, a human volunteer study (clinical phase I trial) with ^{18}F-LMI1195 demonstrated promising clinical results, with uniform myocardial tracer uptake in the left ventricular wall and acceptable radiation exposure (*5*). Further mechanistic details of ^{18}F-LMI1195 cardiac retention are not yet fully elucidated. Understanding the uptake and retention kinetics at a subcellular level is essential in the design of clinical imaging protocols and in the interpretation of imaging results. In this study, we evaluated the in vivo cardiac retention kinetics of this novel PET sympathetic nerve tracer by directly comparing it with the conventional tracers ^{123}I-MIBG and ^{11}C-hydroxyephedrine in rabbit hearts (Fig. 1).

MATERIALS AND METHODS

Radiopharmaceuticals

The ^{123}I-MIBG (AdreView; GE Healthcare) had a specific activity of 74 MBq (2 mCi)/mL and a radiochemical purity of more than 95%. ^{18}F-LMI1195 and ^{11}C-hydroxyephedrine were both synthesized following described procedures (*4,6*). Analyses at the end of syntheses revealed specific radioactivity greater than 10 GBq/μmol and radiochemical purity greater than 95% for both radiolabeled compounds.

Animal Studies

Healthy New Zealand White rabbits (Charles River Laboratories Inc.) weighing 2.3 ± 0.8 kg were used. The animal protocols were approved by the local institutional animal care and use committee and were conducted strictly according to the *Guide for the Care and Use of Laboratory Animals* (*7*). Group sizes corresponded to the biometrical calculations provided in the relevant animal license.

The animals were studied with ^{18}F-LMI1195 PET, ^{11}C-hydroxyephedrine PET, and ^{123}I-MIBG planar scintigraphy under 3 different medications: intravenous pretreatment with the NET inhibitor desipramine, 1.5 mg/kg, 10 min before tracer injection ($n = 3$); a desipramine chase of 1.5 mg/kg, administered 10 min after tracer delivery ($n = 4$); and saline pretreatment of controls ($n = 4$).

Imaging Protocols

All animals were maintained under anesthesia with 2% isoflurane throughout the imaging procedure. Imaging with ^{18}F-LMI1195 and ^{11}C-hydroxyephedrine was performed using a dedicated small-animal PET system (Inveon; Siemens Healthcare). Its characteristics have been described previously (*8,9*). Just before a bolus tracer injection (^{11}C-hydroxyephedrine, 50 MBq; ^{18}F-LMI1195, 50 MBq) via the ear vein, a list-mode 40-min image acquisition was started. The list-mode data were reconstructed into a dynamic sequence (25 frames: 15 × 8 s, 3 × 60 s, 7 × 300 s) using ordered-subset expectation maximization with 16 subsets and 4 iterations. The reconstructed PET images were analyzed using an image-processing application (AMIDE-bin, version 1.0.2) (*10*). Regions of interest were drawn manually on the left ventricular wall, and decay-corrected time–activity curves were generated. The tracer washout rate (%/min) was calculated as follows: {([cardiac counts$_{10\ min}$ − cardiac counts$_{35\ min}$]/cardiac counts$_{10\ min}$) × 100/25 (min)}.

Planar ^{123}I-MIBG imaging was performed using a clinical dual-head γ camera (Symbia E; Siemens Healthcare) equipped with a medium-energy collimator. The animals were placed prone on one detector head. Ten-minute planar acquisitions were started 10 min (early) and 2.5 h (delayed) after ^{123}I-MIBG (50 MBq) injection via the ear vein (128 × 128 matrices, a photopeak window set at 15% around 159 keV). Heart-to-mediastinum ratios were calculated by dividing the count density of the manually drawn region of interest on the left ventricle by that on the mediastinum.

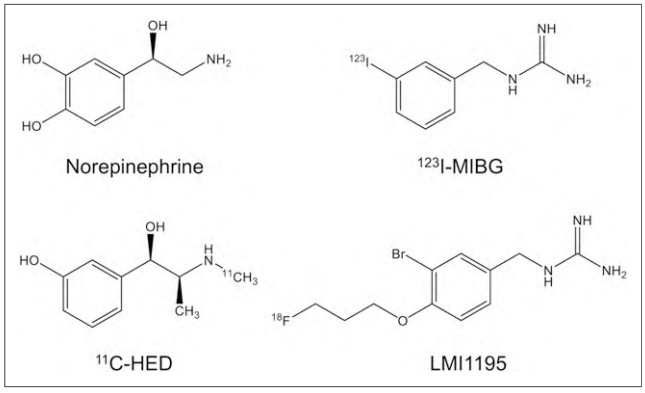

FIGURE 1. Chemical structures of the neurotransmitter norepinephrine, the sympathetic nerve radiotracer ^{18}F-LMI1195, and the conventional tracers ^{123}I-MIBG and ^{11}C-hydroxyephedrine (^{11}C-HED).

Statistical Analysis

All results are displayed as mean ± SD. The 2-tailed paired Student *t* test was used to compare differences between 2 dependent groups, and the 2-tailed independent Student *t* test was used to compare differences between independent groups. A *P* value of less than 0.05 was assumed to be statistically significant. Statistical analysis was done with StatMate III (ATMS Co., Ltd.).

RESULTS

Cardiac Uptake of ^{18}F-LMI1195

^{18}F-LMI1195 PET images of control animals demonstrated clear visualization of the left ventricular wall, with high and homogeneous tracer activity seen throughout the left ventricular myocardium (Fig. 2). Uptake in the surrounding organs, including the liver, remained low compared with the myocardium at 10 and 35 min after tracer injection. Pretreatment with the neural NET inhibitor desipramine reduced cardiac uptake dramatically, and almost no cardiac uptake was identified. In the same way, ^{11}C-hydroxyephedrine cardiac uptake throughout the ventricle was seen in controls and was diminished with desipramine pretreatment. ^{123}I-MIBG planar images also showed focally increased tracer accumulation in the heart, which desipramine pretreatment reduced on the delayed scans (Fig. 3).

Cardiac Retention of ^{18}F-LMI1195

^{18}F-LMI1195 retention in the heart was stable in controls (washout ratio, 0.058% ± 0.28%/min). A NET inhibitor chase with desipramine, added only after initial tracer accumulation, did not change cardiac tracer washout (0.059% ± 0.11%/min, not statistically significant) (Fig. 2). On the other hand, cardiac washout of ^{11}C-hydroxyephedrine was slightly higher than that of ^{18}F-LMI1195 (0.42% ± 0.57%/min) in controls, and washout was further increased by the NET inhibitor chase (2.43% ± 0.15%/min, $P < 0.001$). ^{123}I-MIBG cardiac activity was not influenced by the desipramine chase (delayed heart-to-mediastinum ratio; control and desipramine chase, 2.05 ± 0.16 and 1.99 ± 0.12, respectively, not statistically significant) (Fig. 3).

DISCUSSION

In the present study, we directly compared the uptake kinetics of a new sympathetic nerve tracer, ^{18}F-LMI1195, with the most widely used conventional PET and SPECT tracers (^{11}C-hydroxyephedrine and ^{123}I-MIBG) using pharmacologic interventions with the NET

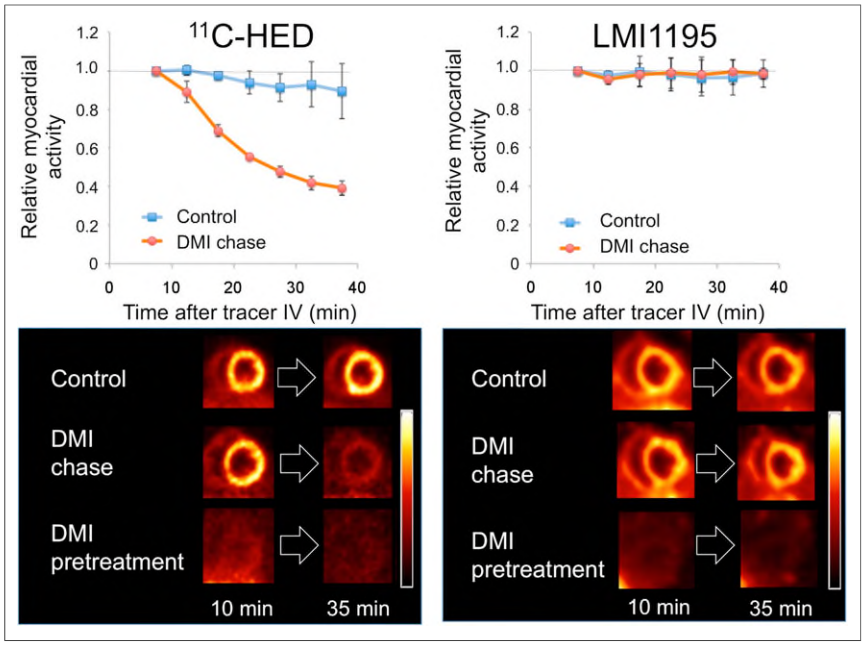

FIGURE 2. Averaged time–activity curves and representative short-axis images of in vivo rabbit cardiac PET imaging. Desipramine (DMI) chase enhanced ^{11}C-hydroxyephedrine (^{11}C-HED) washout from heart, whereas ^{18}F-LMI1195 washout did not change.

inhibitor desipramine. All tested tracers demonstrated feasibility for neural imaging in rabbit hearts, with specific initial uptake via the NET. Interestingly, desipramine—added only after initial tracer distribution as a NET inhibitor chase treatment—demonstrated distinct differences among the tracers (Fig. 4). The ^{11}C-hydroxyephedrine washout from the heart was enhanced by the desipramine chase, suggesting that continuous cyclical release (diffusion out) and reuptake of ^{11}C-hydroxyephedrine via neural NET is occurring to maintain the tracer retention in the heart. In contrast, ^{18}F-LMI1195 and ^{123}I-MIBG cardiac retentions were not influenced by the desipramine chase, demonstrating stable tracer retention in the nerve terminals independent of NET activity after initial transport. Although further confirmation in humans is needed, these basic characteristics of tracer kinetics may be helpful for optimizing clinical protocols and for interpreting imaging results. Furthermore, with an understanding of these basic tracer kinetics, a clinical interpreter could select or even combine more than 2 tracers to gain insight into the specific processes of norepinephrine handling in the nerve terminals (*11*).

Specific tracer uptake via the neural NET system is the most important basic characteristic for imaging presynaptic sympathetic innervation and norepinephrine handling (*12,13*). Desipramine is the most commonly used selective norepinephrine uptake inhibitor for the uptake-1 mechanism at the nerve terminal (*14*). In the present in vivo rabbit study, all tested tracers—^{18}F-LMI1195, ^{11}C-hydroxyephedrine, and ^{123}I-MIBG—had a high affinity for neural uptake as demonstrated by the desipramine blockade. First of all, NET-mediated uptake of ^{18}F-LMI1195 by in vitro cell uptake studies using human neuroblastoma cells demonstrated kinetic values comparable to norepinephrine (*4*). In a subsequent study, ^{18}F-LMI1195 was tested using an isolated perfused rabbit heart system to avoid the effect of systemic recirculation of tracer and tracer metabolites (*15*). First-pass ^{18}F-LMI1195 extraction was measured as 44% and 28% using a flow value of 2 and 4 mL/min/g, respectively. Desipramine added into the perfusion buffer markedly reduced the extraction to 4% at 4 mL/min/g. Furthermore, in vivo PET studies have confirmed the high contrast of ^{18}F-LMI1195 cardiac uptake in rabbits, monkeys, and humans (*4,5*). Notably, the specific neural transport observed in these species is not the same as seen in small rodents (*16,17*). Desipramine treatment did not change the cardiac ^{18}F-LMI1195 uptake in rat hearts, whereas phenoxybenzamine, a potent norepinephrine nonselective NET inhibitor (*18*), significantly reduced the tracer uptake. Therefore, ^{18}F-LMI1195 transport via the extraneural uptake-2 mechanism was suggested and is consistent with transport considerably mediated by uptake-2 in the small rodent hearts. On the other hand, ^{11}C-hydroxyephedrine demonstrated sensitivity for the desipramine treatment even in the in vivo rat heart, whereas ^{123}I-MIBG uptake was not affected in the same way as ^{18}F-LMI1195 uptake (*19*). Consistent with these findings, DeGrado et al. also demonstrated the high affinity of ^{11}C-hydroxyephedrine to uptake-1 using isolated perfused rat hearts (*20*). The precise mechanism of these species- and tracer-dependent uptake variations needs to be further investigated. It is known that there are significant species variations in physiologic norepinephrine handling in the heart (*21*). These include the level of extraneural uptake-2 mechanism, as well as variations in the characteristics of the NET itself.

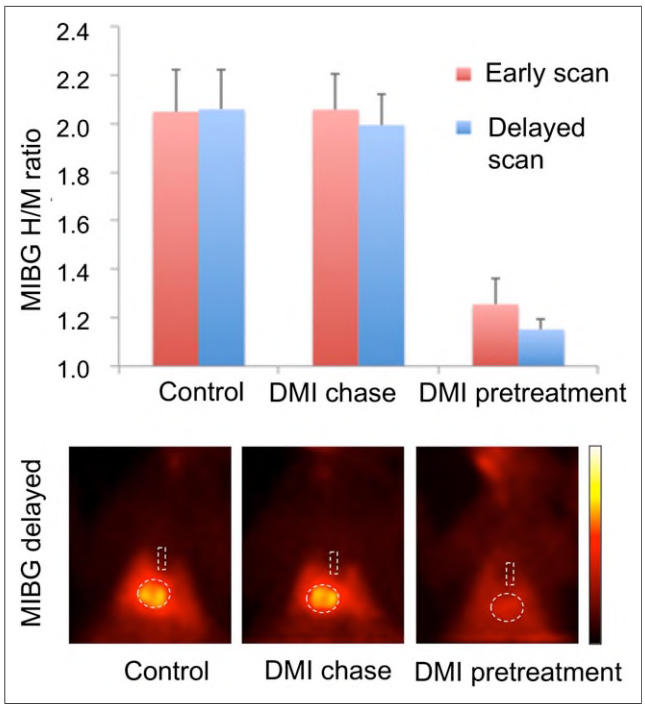

FIGURE 3. Results of in vivo rabbit ^{123}I-MIBG planar scintigraphy of chest. Desipramine (DMI) chase did not change cardiac distribution of ^{123}I-MIBG. Dotted lines indicate regions of interest in heart and mediastinum. H/M ratio = heart-to-mediastinum ratio.

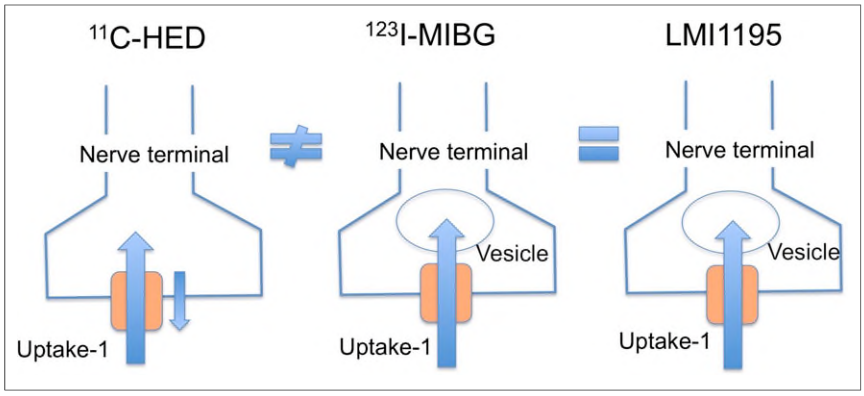

FIGURE 4. Simplified schematic of ^{11}C-hydroxyephedrine (^{11}C-HED), ^{123}I-MIBG, and ^{18}F-LMI1195 kinetics at nerve terminals. After transportation into nerve terminals via uptake-1 NET system, ^{11}C-hydroxyephedrine retention is maintained by continuous uptake-1 activity, whereas ^{18}F-LMI1195 and ^{123}I-MIBG seem to be stored stably at nerve terminals.

Although all available presynaptic sympathetic nerve norepinephrine analog tracers are designed to be initially transported into nerve terminals to visualize the nervous system, significant differences in intraneural kinetics have been reported among these tracers (*22,23*). Understanding this subcellular tracer handling is essential for fundamental interpretation of the imaging results. To investigate the retention mechanism, we tested 3 tracers with a neural NET inhibitor chase treatment; therefore, desipramine was added only at the washout phase just after initial tracer uptake.

Increased tracer washout from the heart after a desipramine chase was observed for ^{11}C-hydroxyephedrine. This result is consistent with earlier studies performed with isolated perfused rat hearts and in vivo rat imaging (*20,24*). These findings indicate that ^{11}C-hydroxyephedrine cardiac retention is maintained by continuous reuptake via NET and release (diffusion) from the nerve terminals. Norepinephrine is stored in the synaptic vesicles at nerve terminals, and when a firing impulse arrives at the synaptic ending, the sympathetic nerve neurotransmitter norepinephrine is released into the synaptic cleft via vesicular exocytosis. ^{11}C-hydroxyephedrine cardiac retention reflects NET reuptake activity, while being less influenced by this vesicular turnover.

In contrast, ^{18}F-LMI1195, similar to ^{123}I-MIBG, demonstrated stable tracer retention resistant to the NET inhibitor chase treatment. ^{18}F-LMI1195 and ^{123}I-MIBG share a benzylguanidine structure (Fig. 1), possibly explaining the similarity of response to the desipramine chase. Consistent with these findings, isolated perfused rabbit heart experiments demonstrated no effect from the addition of desipramine to the perfusion buffer after the tracer uptake phase (*15*). This indicates stable tracer retention independent of NET activity. Furthermore, electrical field stimulation enhanced cardiac ^{18}F-LMI1195 washout significantly in the isolated rabbit heart study (*15*). The stimulation is known to evoke norepinephrine overflow via vesicular release into the synaptic cleft at the nerve terminals (*25*). Therefore, the enhanced ^{18}F-LMI1195 washout by the electrical provocation suggests the possibility of ^{18}F-LMI1195 storage in the synaptic vesicle.

Integrating the available information, ^{18}F-LMI1195 is most likely to be readily transported and stored into synaptic vesicles after being taken up into the nerve terminals, mimicking the norepinephrine vesicular turnover pathway. Thereby, dynamic ^{18}F-LMI1195 PET to measure tracer washout kinetics would provide parameters not only for uptake-1 function but also for sympathetic afferent activity correlated with norepinephrine spillover from the heart. Although further confirmatory experiments are required, such as reserpine (vesicular transport inhibitor) blocking studies to exclude the possibility of nonspecific localization in intraneuronal membranes, our study demonstrates the potential of ^{18}F-LMI1195 for monitoring the handling of norepinephrine at the sympathetic nerve terminals, including vesicular turnover at the myocardium.

CONCLUSION

^{18}F-LMI1195, a novel ^{18}F-labeled benzylguanidine analog PET tracer, demonstrates specific uptake in the heart as assessed by in vivo PET imaging in rabbits. Stable retention under a desipramine chase indicates promising properties as a new class of PET tracer for visualizing the cardiac nervous system, mimicking physiologic norepinephrine turnover at nerve terminals.

DISCLOSURE

The costs of publication of this article were defrayed in part by the payment of page charges. Therefore, and solely to indicate this fact, this article is hereby marked "advertisement" in accordance with 18 USC section 1734. This work was supported by the Competence Network of Heart Failure funded by the Integrated Research and Treatment Center (IFB) of the Federal Ministry of Education and Research (BMBF) and German Research Council (DFG grant HI 1789/2-1). No other potential conflict of interest relevant to this article was reported.

REFERENCES

1. Parati G, Esler M. The human sympathetic nervous system: its relevance in hypertension and heart failure. *Eur Heart J.* 2012;33:1058–1066.
2. Jacobson AF, Senior R, Cerqueira MD, et al. Myocardial iodine-123 meta-iodobenzylguanidine imaging and cardiac events in heart failure: results of the prospective ADMIRE-HF (AdreView Myocardial Imaging for Risk Evaluation in Heart Failure) study. *J Am Coll Cardiol.* 2010;55:2212–2221.
3. Fallavollita JA, Heavey BM, Luisi AJ Jr, et al. Regional myocardial sympathetic denervation predicts the risk of sudden cardiac arrest in ischemic cardiomyopathy. *J Am Coll Cardiol.* 2014;63:141–149.
4. Yu M, Bozek J, Lamoy M, et al. Evaluation of LMI1195, a novel ^{18}F-labeled cardiac neuronal PET imaging agent, in cells and animal models. *Circ Cardiovasc Imaging.* 2011;4:435–443.
5. Sinusas AJ, Lazewatsky J, Brunetti J, et al. Biodistribution and radiation dosimetry of LMI1195: first-in-human study of a novel ^{18}F-labeled tracer for imaging myocardial innervation. *J Nucl Med.* 2014;55:1445–1451.
6. Rosenspire KC, Haka MS, Van Dort ME, et al. Synthesis and preliminary evaluation of carbon-11-meta-hydroxyephedrine: a false transmitter agent for heart neuronal imaging. *J Nucl Med.* 1990;31:1328–1334.
7. *Guide for the Care and Use of Laboratory Animals*. 8th ed. Washington, DC: National Academies Press; 2011.
8. Yamane T, Park MJ, Richter D, et al. Small-animal PET imaging of isolated perfused rat heart. *J Nucl Med.* 2014;55:495–499.
9. Disselhorst JA, Brom M, Laverman P, et al. Image-quality assessment for several positron emitters using the NEMA NU 4-2008 standards in the Siemens Inveon small-animal PET scanner. *J Nucl Med.* 2010;51:610–617.

10. Loening AM, Gambhir SS. AMIDE: a free software tool for multimodality medical image analysis. *Mol Imaging.* 2003;2:131–137.
11. Lautamaki R, Sasano T, Higuchi T, et al. Multiparametric molecular imaging provides mechanistic insights into sympathetic innervation impairment in the viable infarct border zone. *J Nucl Med.* 2015;56:457–463.
12. Higuchi T, Schwaiger M. Noninvasive imaging of heart failure: neuronal dysfunction and risk stratification. *Heart Fail Clin.* 2006;2:193–204.
13. Higuchi T, Schwaiger M. Imaging cardiac neuronal function and dysfunction. *Curr Cardiol Rep.* 2006;8:131–138.
14. Foley KF, Cozzi NV. Inhibition of transport function and desipramine binding at the human noradrenaline transporter by N-ethylmaleimide and protection by substrate analogs. *Naunyn Schmiedebergs Arch Pharmacol.* 2002;365: 457–461.
15. Higuchi T, Yousefi BH, Reder S, et al. Myocardial kinetics of a novel [^{18}F]-labeled sympathetic nerve PET tracer LMI1195 in the isolated perfused rabbit heart. *JACC Cardiovasc Imaging.* March 12, 2015 [Epub ahead of print].
16. Higuchi T, Yousefi BH, Kaiser F, et al. Assessment of the ^{18}F-labeled PET tracer LMI1195 for imaging norepinephrine handling in rat hearts. *J Nucl Med.* 2013;54: 1142–1146.
17. Yu M, Bozek J, Kagan M, et al. Cardiac retention of PET neuronal imaging agent LMI1195 in different species: impact of norepinephrine uptake-1 and -2 transporters. *Nucl Med Biol.* 2013;40:682–688.
18. Iversen LL, Salt PJ, Wilson HA. Inhibition of catecholamine uptake in the isolated rat heart by haloalkylamines related to phenoxybenzamine. *Br J Pharmacol.* 1972;46:647–657.
19. Rischpler C, Fukushima K, Isoda T, et al. Discrepant uptake of the radiolabeled norepinephrine analogues hydroxyephedrine (HED) and metaiodobenzylguanidine (MIBG) in rat hearts. *Eur J Nucl Med Mol Imaging.* 2013;40:1077–1083.
20. DeGrado TR, Hutchins GD, Toorongian SA, Wieland DM, Schwaiger M. Myocardial kinetics of carbon-11-meta-hydroxyephedrine: retention mechanisms and effects of norepinephrine. *J Nucl Med.* 1993;34:1287–1293.
21. Jarrott B. Uptake and metabolism of catecholamines in the perfused hearts of different species. *Br J Pharmacol.* 1970;38:810–821.
22. Raffel DM, Wieland DM. Assessment of cardiac sympathetic nerve integrity with positron emission tomography. *Nucl Med Biol.* 2001;28:541–559.
23. Bengel FM. Imaging targets of the sympathetic nervous system of the heart: translational considerations. *J Nucl Med.* 2011;52:1167–1170.
24. Tipre DN, Fox JJ, Holt DP, et al. In vivo PET imaging of cardiac presynaptic sympathoneuronal mechanisms in the rat. *J Nucl Med.* 2008;49:1189–1195.
25. Kreusser MM, Haass M, Buss SJ, et al. Injection of nerve growth factor into stellate ganglia improves norepinephrine reuptake into failing hearts. *Hypertension.* 2006;47:209–215.